Asian Journal of Chemistry Vol. 21, No. 4 (2009), 2745-2754

Microwave-Assisted Hydrothermal Synthesis of SBA-15 Molecular Sieve

HUI YU and QING-ZHOU ZHAI*
Research Center for Nanotechnology, Changchun University of Science and Technology, Changchun 130022, Jilin Province, P.R. China
Fax: (86)(431)85383815; Tel: (86)(431)85583118
E-mail: zhaiqingzhou@163.com; zhaiqingzhou@hotmail.com

In the present study, SBA-15 molecular sieve was successfully synthesized by a microwave-assisted hydrothermal synthesis method, using poly(ethylene glycol)-block-poly(propyl glycol)-block-poly(ethylene glycol) ($EG_{20}PG_{40}EG_{20}$) as a template. The time of synthesis of SBA-15 molecular sieve by microwave-assisted hydrothermal synthesis method only needs 125 min, synthetical speed is 34 times faster than that by the conventional hydrothermal synthesis method. The results showed that the primary particles of the samples present acicular crystals. The longness is 100 μm for SBA-15 sample synthesized by microwave method in 5 min (S_1) and 64 μm for SBA-15 sample synthesized by microwave method in 0.5 h (S_2), respectively. The diameters are 4.5 μm for S_1 sample and 3.6 μm for S_2 sample, respectively. These data showed that the sizes of the SBA-15 molecular sieve synthesized by present method were much bigger than those by the conventional hydrothermal synthesis method and by the other microwave-assisted hydrothermal synthesis methods.

Key Words: SBA-15 molecular sieve, $EG_{20}PG_{40}EG_{20}$ template, Microwave-assisted synthesis, Characterization.

INTRODUCTION

For molecular sieves, conventional synthesis methods (For example, hydrothermal synthesis method and vapour phase transport method) need long crystallization times *i.e.*, few hours to few days. The long crystallization time usually results in the formation of impure molecular sieve[1]. Because of the low heating rate and inhomogeneous heating, molecular sieve nuclei do not form on the support surface simultaneously and molecular sieve crystals are not uniform in size[2,3]. Recently, a new synthesis method that combines hydrothermal crystallization with a microwave heating technique has been developed. The microwave-assisted synthesis of molecular sieves is relatively new area of research. The term microwave-assisted hydrothermal synthesis (MAHS) process was proposed by Komarneni *et al.*[4] and this process has been used for the rapid synthesis of numerous ceramic oxides,

hydroxylated phases, porous materials and metal powders. Recently, the microwave-assisted hydrothermal synthesis (MAHS) method has been successfully applied to synthesize some molecular sieves, such as $AlPO_4$-5[5], Beta[6], MCM-41[7], Y[8], ZSM-5[8] and $AlPO_4$-11[9]. Energy transfer from microwaves to the materials is believed to occur either through resonance or relaxation, which results in rapid heating. Furthermore, during the synthesis of nanoporous materials, an employment of microwave technique shows versatile good effects, for instance, (1) Short heating times. (2) Inductive heating through the conducting properties of the synthesis mixture. (3) Specific energy dissipation *via* microwave energizes the hydroxylated surface or associated water molecules in the boundary layer, forming the active water molecules with the high potential[10-13]. Microwave-assisted synthesis of molecular sieves offers many distinct advantages over conventional synthesis. They include rapid heating to crystallization temperature due to volumetric heating resulting in homogeneous nucleation, fast supersaturation by the rapid dissolution of precipitated gels and eventually a shorter crystallization time compared to conventional autoclave heating. Furthermore, MAHS method of molecular sieve has the advantages of broad synthesis composition, narrow particle size distribution and high purity[2] and it is energy efficient and economical[14]. These advantages prompt researchers to explore its use as a method for the synthesis of molecular sieves.

SBA-15 molecular sieve is a material that has a 2D hexagonal arrangement of pores. It has the benefits of a combined microporosity and mesoporosity and relatively thick walls[15]. The enhanced chemical and thermal stability of these materials as compared with MCM-41 can be ascribed to the thicker pore walls in the SBA-15 materials and attracts much interest[16]. SBA-15 molecular sieve is usually obtained by hydrothermal reaction in a period of several days using tetraethyl orthosilicate (TEOS) as the silica source and triblock organic copolymer as the structure-directing agent. Newalker and his co-workers[14,17] reported successful synthesis of SBA-15 molecular sieve using a triblock organic copolymer as a template under microwave-hydrothermal conditions within 2 h. Then, they studied the effect of salt for SBA-15 framework during synthesis of SBA-15 molecular sieve by microwave-hydrothermal method[17]. In microwave a long time may destroy framework of SBA-15 molecular sieve and decrease the purity of SBA-15. In the present study, SBA-15 molecular sieve has been successfully synthesized using poly(ethylene glycol)-block-poly(propyl glycol)-block-poly(ethylene glycol) ($EG_{20}PG_{40}EG_{20}$) as a template under microwave-hydrothermal conditions within about 5 min and synthesis is more than 34 times faster than by the conventional hydrothermal synthesis method[15].

EXPERIMENTAL

Tetraethyl orthosilicate (TEOS, 98 %, Fluka), poly(ethylene glycol)-block-poly(propylene glycol)-block-poly(ethylene glycol) ($EG_{20}PG_{40}EG_{20}$, Aldrich) and 2 mol L^{-1} hydrochloric acid (AR) solution was used and the water used in experiments was deionized water.

Synthesis of SBA-15 molecular sieve by microwave-hydrothermal synthesis method: Microwave-hydrothermal synthesis of SBA-15 molecular sieve was performed using a LG WD900 [MG-5515SD, LG Electronics (Tianjin) Appl. Co., Ltd., China] domestic microwave ovens. The experiment was operated under a maximum power of 1200 W and a microwave frequency of 2.45 GHz.

Mesoporous SBA-15 molecular sieve was prepared according to the procedure as follows: 2.0 g of $EG_{20}PG_{40}EG_{20}$ was dissolved in 60 g of 2 mol L^{-1} hydrochloric acid and 15.0 g of deionized water. Finally, 4.25 g TEOS was added into the homogeneous solution with stirring to form a reactive gel at 40 ºC. The obtained gel was heated in Teflon-liner autoclaves under a power of 1200 W and a microwave frequency of 2.45 GHz for 5 and 30 min, respectively. The samples were designed as S_1 and S_2, respectively. The products were filtered and washed with deionized water and dried in room temperature. The obtained materials were calcined at 550 °C for 24 h to eliminate the template. The white powers were obtained.

Characterization: X-ray powder diffraction (XRD) patterns were collected on a Siemens D5005 diffractometer using Cu-Kα radiation (λ = 1.5418 Å and operating at 30 kV and 20 mA). Fourier transform infrared (FT-IR) spectra were obtained using a Bruker Vertex 70 FT-IR spectrometer. Powder samples (1 % wt) were dispersed in KBr (99 % wt) pellets for IR analysis. Adsorption-desorption studies of nitrogen were performed on a Micromeritics ASAP 2010M volumetric adsorption analyzer at 77 K. A sample was degassed in vacuum at 573 K for 12 h before measurement. Surface areas were calculated based on the BET (Brunner-Emmett-Teller) method[18], while pore size distribution was computed using the BJH (Barrett-Joyner-Halenda) method[19]. Transmission electron microscopy (TEM) images were taken on a Jeol 2010 TEM instrument. Scanning electron microscopy (SEM) images were recorded on a Jeol JSM-5600L SEM instrument.

RESULTS AND DISCUSSION

Powder X-ray diffraction (XRD): Fig. 1 shows the small-angle XRD patterns of the samples of S_1, S_2 and SBA-15 synthesized by conventional hydrothermal method. These samples possess 4 reflection peaks,which are denoted as (100), (110), (200) and (210), respectively. These peaks belong to those of SBA-15 molecular sieve[15]. The four characteristic peaks of SBA-15 molecular sieve structure indicate the 2-D hexagonal pore structure (P6mm) of SBA-15 and the SBA-15 molecular sieve keeps much highly ordered state. It shows that its damage to SBA-15 molecular sieve by microwave-assisted synthesis method is small and its crystallization degree is higher than conventional way, contrarily. The peaks of (100) reflections of S_1 and S_2 shift to smaller angles in comparison with the conventional way sample (Fig. 1), which locates at $2\theta = 0.84°$ for conventional way, $2\theta = 0.78°$ for both microwave-assisted synthesis methods, respectively. It is counted d_{100} = 10.52 nm, (unit cell parameter a_0 = 12.15 nm) for the samples by conventional method, but d_{100} = 11.33 nm (unit cell parameter a_0 = 13.08 nm) for the samples by microwave-assisted synthesis methods.

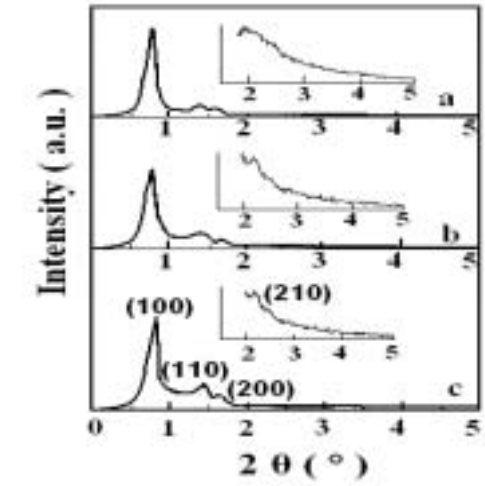

Fig. 1. Small-angle XRD patterns of: a) S_1 (Microwave-assisted synthesis of SBA-15 molecular sieve in 5 min), b) S_2 (Microwave-assisted synthesis of SBA-15 molecular sieve in 0.8 h), c) SBA-15 (Hydrothermal synthesis)

Fourier transform infrared (FT-IR) spectra: Infrared spectra can reflect configuration of the frameworks of molecular sieve. Fig. 2 shows the FT-IR spectra of each sample. In the FT-IR patterns, each sample has four peaks. The bands that locate at 458, 459, 460 cm^{-1} correspond to T-O bending. The bands that locate at 804, 809, 802 cm^{-1} correspond to symmetric stretching. The bands that locate at 963, 970, 962 and 1089, 1086, 1090 cm^{-1} correspond to asymmetric stretching[20]. The peaks that locate at 963, 970, 962 cm^{-1} are also assigned to the stretching of non-bridging oxygen atoms of Si-OH.

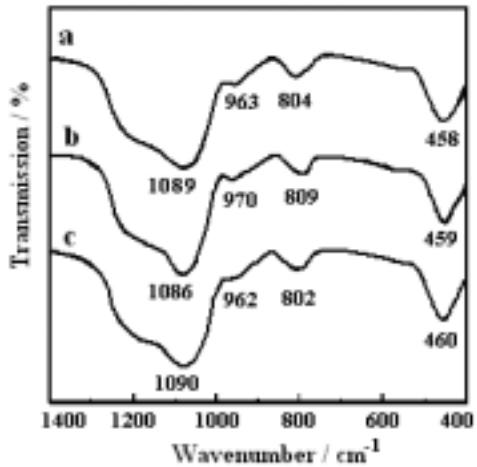

Fig. 2. Infrared spectra of the samples (a) S_1 (Microwave-assisted synthesis of SBA-15 molecular sieve in 5 min), b) S_2 (Microwave-assisted synthesis of SBA-15 molecular sieve in 0.5 h), c) SBA-15 (Hydrothermal synthesis)

Low temperature nitrogen adsorption-desorption isotherms: Fig. 3A shows the low temperature nitrogen adsorption-desorption isotherms of the samples. The isotherms of all samples show typical irreversible type IV adsorption isotherms with a H1 hysteresis loop which are characteristic of mesoporous materials with 1-D cylindrical channels as defined by IUPAC[21]. The isotherms of the samples featured hysteresis loops with sharp adsorption and desorption branches. The sharpness of the adsorption branches is indicative of a narrow mesopore size distribution (Fig. 3B). At low partial pressures (P/P_0), the adsorption is mainly monolayer adsorption. There is no pore-blocking effects from narrow pores during desorption and the capillary condensation can not occur at relative lower pressures. Therefore hysteresis feature does not appear. The adsorption is multilayer adsorption as relative pressure increases and adsorptive quantity increases. However, the volumes adsorbed inflected sharply at relative pressure (p/p_0) 0.73 for the SBA-15 molecular sieve by conventional synthesis method, 0.70 for S_1, 0.65 for S_2, respectively. It can be explained that the relative pressure increased to the degree that capillary condensation occur. The difference between adsorption and desorption process can conclude that adsorption and desorption are irreversible, desorption lag to adsorption process. The most possible reason is due to the effect of constrictions in the cylindrical mesopores, which would cause the delayed capillary evaporation[22,23]. Thus, adsorption process and desorption process may progress under the different relative pressure[24]. In the case of mesopores, the capillary condensation pressure is an increasing function of the pore diameter. When the relative pressure is higher than 0.85 for the SBA-15 molecular sieve by conventional synthesis method, 0.83 for S_1 and 0.84 for S_2, the hysteresis does not appear. It is because adsorption process and desorption process mainly carries out on the out surface and the process is reversible.

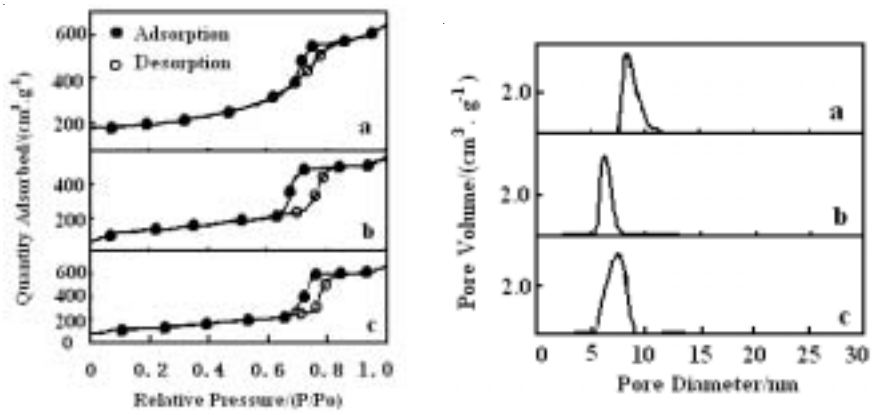

(A) (B)

Fig. 3. A. Low temperature nitrogen adsorption-desorption isotherms (• adsorption; o desorption)
B. Pore size distribution patterns of samples (a) SBA-15 (Hydrothermal synthesis), (b) Microwave-assisted synthesis of SBA-15 molecular sieve in 5 min (S_1), (c) Microwave-assisted synthesis of SBA-15 molecular sieve in 0.5 h (S_2)

The calculated BET surface areas and the mesopore parameters based on the Barrett, Joyner and Halenda (BJH)[18,19] analysis are calculated from the adsorption branch of nitrogen adsorption-desorption isotherms. As show in Table-1, for the SBA-15 molecular sieve by conventional synthesis method, S_1 and S_2, the average pore diameters is 8.14, 6.49 and 7.40 nm, the BET surface is 594.7, 536.3 and 564.3 $m^2 g^{-1}$, the pore volume is 1.059, 0.871 and 1.044 $cm^3 g^{-1}$, respectively. The relative condensation pressure, which is a function of pore diameter, was found to increase with an increase in crystallization time which in turn reflected an increase in pore dimension and a decrease in silica wall thickness, accordingly, an increase in the BET surface and the pore volume. These results are in good agreement with those reported under the conventional hydrothermal route[25] and may be due to the rapid dehydration of EG blocks of the copolymer[26] at 373 K as a function of time under microwave-hydrothermal conditions[14].

TABLE-1
PORE STRUCTURE PARAMETERS OF SAMPLES

Sample	d_{100} (nm)	a_0[a] (nm)	BET surface area ($m^2 g^{-1}$)	Pore volume[b] ($cm^3 g^{-1}$)	Pore size[c] (nm)
S	10.52	12.15	594.7	1.059	8.14
S_1	11.33	13.08	536.3	0.871	6.49
S_2	11.33	13.08	564.3	1.044	7.40

[a] $a_0 = \frac{2}{\sqrt{3}} d_{100}$, [b]BJH adsorption cumulative volume of pores,
[c]Pore size calculated from the adsorption branch.

Transmission electron microscopy (TEM): Fig. 4-A-a, Fig. 4-B-a and Fig. 4-C-a show the TEM images of the samples which were taken with the beam direction parallel to the pores. Fig. 4-A-b, Fig. 4-B-b and Fig. 4-C-b show the TEM images of the samples which were taken with the beam direction perpendicular to the pores. All micrographs are recorded with the electron beam direction parallel to and perpendicular to the channel direction. TEM experiments show the well-ordered hexagonal arrays of mesopores and straight lattice fringes seen from the images viewed along and perpendicular to the pore axis, confirming the existence of a 2-D hexagonal structure of a p6mm symmetry.

Scanning electron microscopy (SEM): Fig. 5 shows SEM images of the samples. SEM analyses of the samples show that the primary particles of the samples present acicular crystals for the SBA-15 molecular sieve synthesized by present method and fibriform crystals for the SBA-15 molecular sieve by conventional synthesis method. The crystals longness is 727 nm for the SBA-15 molecular sieve by conventional synthesis method, 100 μm for S_1 sample and 64 μm for S_2 sample. The crystals diameter is 333 nm for the SBA-15 molecular sieve by conventional synthesis method, 4.5 μm for S_1 sample and 3.6 μm for S_2 sample. The SBA-15 molecular sieve crystals by conventional synthesis method have a smaller crystal size than those of S_1 and S_2 samples.

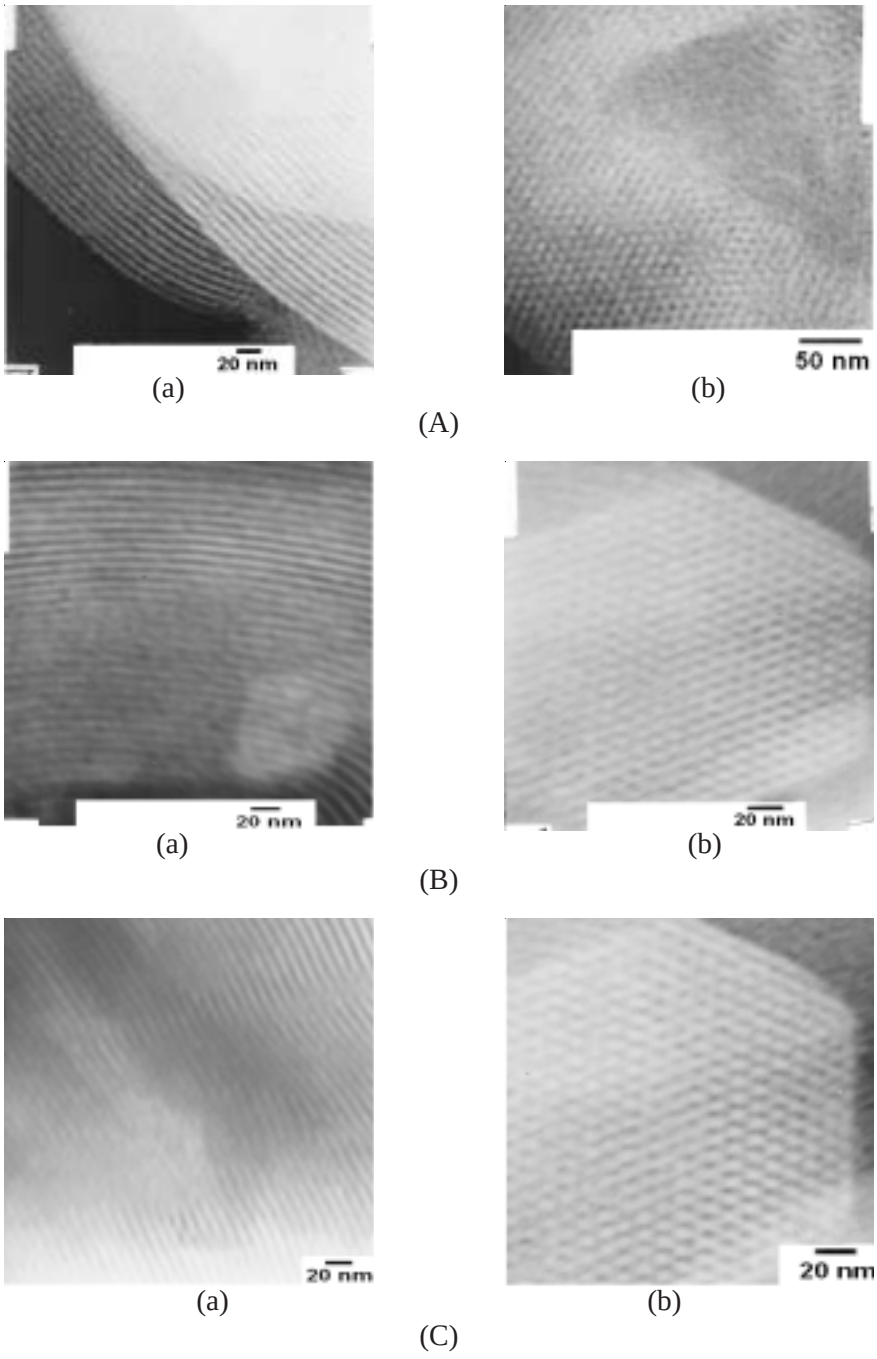

Fig. 4. TEM images of the samples (a) taken with the beam direction parallel to the pores and (b) taken with the beam direction perpendicular to the pores. (A) SBA-15 (Hydrothermal synthesis), (B) Microwave-assisted synthesis of SBA-15 molecular sieve in 5 min (S_1), (C) Microwave-assisted synthesis of SBA-15 molecular sieve in 0.5 h (S_2)

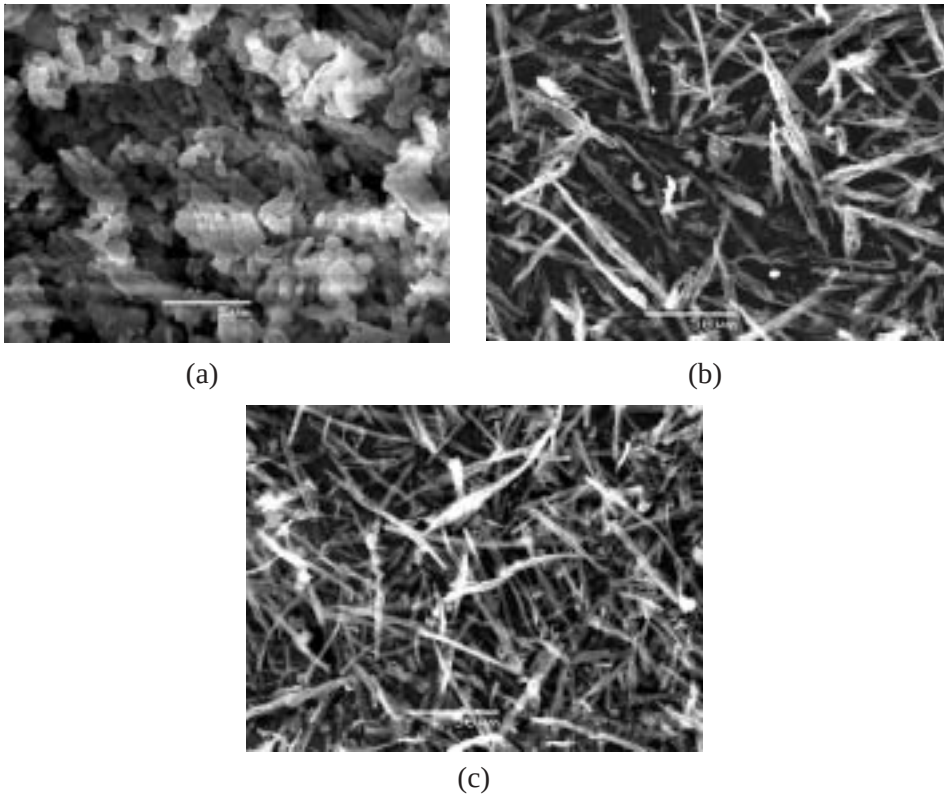

Fig. 5. SEM images of the samples (a) Hydrothermal synthesis of SBA-15, (b) Microwave-assisted synthesis of SBA-15 molecular sieve in 5 min (S_1), (c) Microwave-assisted synthesis of SBA-15 molecular sieve in 0.5 h (S_2)

Theoretical analysis of synthesis process: The microwave energy speeds up the formation of intermediates of surfactant and silica precursors and their assembly on templates[27]. For nonionic surfactant ($EG_{20}PG_{40}EG_{20}$), the increase in PG chain length of surfactant molecule results in increasing the *d*-spacing and pore volume. But the increase in EG chain length makes the pore volume reduce and the *d*-spacing does not increase. In addition, the enhanced Brownian motion and the rotational dynamics of the water molecules may intervene in the mechanism of microstructure formation in variable stages of each process. In fact, water molecules strongly absorb microwave energy due to their high dielectric constant, yielding so-called active water with high mobility[8]. In other words, the microwave irradiation may destroy the hydrogen bridges of the water molecules by ion oscillation and water dipole rotation and produce the active water[28]. In microwave synthesis of molecular sieves, the reduction in the crystallization period is generally considered to result from the high potential of the active water to dissolve the gel constituents under microwave irradiation[8]. The lone pair of a hydroxyl group of the active water

molecules was reported to have higher potential to dissolve the gel constituents than normal water[6]. This environment provides more opportunity for the rapid formations of multiply charged silicate oligomers such as double three-ring (D3R) or double four-ring (D4R) species, which can be used to initiate mesophase assembly accelerating the interaction between surfactants and hydrolyzed products of silicate at the interface. Therefore, it is believed that microwave heating not only adds heat energy, but also affects the initial stage of the mesophase formation, since continuous and longer microwave treatment causes the metastable mesophase to collapse into disordered channels and finally form an amorphous structure.

Conclusion

This work shows that SBA-15 molecular sieve has been rapidly synthesized by microwave method. Under microwave irradiation, the induction period shortens in the nucleation step for rapid synthesis of the material. The synthesis of the SBA -15 molecular sieve by MAHS method needs only 125 min which is faster 34 times than by the conventional hydrothermal synthesis method. The average pore diameters are 6.45 nm for S_1 and 7.40 nm for S_2, respectively. The BET surface is 536.3 $m^2 g^{-1}$ for S_1 and 564.3 $m^2 g^{-1}$ for S_2. The pore volume is 0.871 $cm^3 g^{-1}$ for S_1 and 1.044 $cm^3 g^{-1}$ for S_2. The primary particles of the samples present acicular crystals, their longness is 100 μm for S_1 sample and 64 μm for S_2 sample. Their diameter is 4.5 μm for S_1 sample and 3.6 μm for S_2 sample. These data show that the crystals of the SBA-15 molecular sieve synthesized by present method are much bigger than those by the conventional hydrothermal synthesis method and by the other MAHS methods.

ACKNOWLEDGEMENT

The authors are grateful to the financial support (Grant No.: XJJ2005-09) from Changchun University of Science and Technology, P. R. China.

REFERENCES

1. X.C. Xu, W.S. Yang, J. Liu and L.W. Lin, *Micropor. Mesopor. Mater.*, **43**, 299 (2001).
2. X.C. Xu, W.S. Yang, J. Liu and L.W. Lin, *Adv. Mater.*, **12**, 195 (2000).
3. X.C. Xu, W.S. Yang, J. Liu and L.W. Lin, *Sep. Purfi. Technol.*, **25**, 241 (2001).
4. S. Komarneni, R. Roy and Q.H. Li, *Mater. Res. Bull.*, **27**, 1393 (1992).
5. I. Girnus, K. Jancke, R. Vetter, J.R. Mendau and J. Caro, *Zeolites*, **15**, 33 (1995).
6. D.S. Kim, J.S. Chang, H. Wang, S.E. Park and J.M. Kim, *Micropor. Mesopor. Mater.*, **68**, 77 (2004).
7. C.G. Wu and T. Bein, *Chem. Commun.*, **8**, 925 (1996).
8. A. Arafat, J.C. Jansen, A.R. Ebaid and V.H. Bekkum, *Zeolites*, **13**, 162 (1993).
9. M. Park and S. Komarneni, *Micropor. Mesopor. Mater.*, **20**, 39 (1998).
10. P. Chu, F.G. Dwyer and J.C. Vartuli, Crystallization Method Using Microwave Radiation[P], US Patent Application, NO. 4 778 666, (1988).
11. S.E. Park, D.S. Kim, J.S. Chang and W.Y. Kim, *Catal. Today*, **44**, 301 (1998).
12. C.S. Cundy, *Coll. Czech. Chem. Commun.*, **63**, 1699 (1998).
13. S.E. Park, Y.K. Hwang, D.S. Kim, S.H. Jhung, J.S. Hwang and J.S. Chang, *Catal. Surve. Asia*, **8**, 90 (2004).

14. B.L. Newalkar, S. Komarneni and H. Katsuki, *Chem. Comm.*, 2389 (2000).
15. D.Y. Zhao, J.L. Feng, Q.S. Huo, N. Melosh, G.H. Fredrickson, B.F. Chmelka and G.D. Stucky, *Science*, **279**, 548 (1998).
16. P.V.D. Voort, P.I. Ravikovitch, K.P.D. Jong, A.V. Neimark, A.H. Janssen, Benjelloun, E.V. Bavel, P. Cool, B.M. Weckhuysen and E.F. Vansant, *Chem. Commun.*, 1010 (2002).
17. B.L. Newalkar and S. Komarneni, *Chem. Commun.*, 1774 (2002).
18. S. Brunauer, P.H. Emmett and E. Teller, *J. Am. Chem. Soc.*, **60**, 309 (1938).
19. E.P. Barrett, L.G. Joyner and P.P. Halenda, *J. Am. Chem. Soc.*, **73**, 373 (1951).
20. S.Y. Yu, L.P. Wang, B. Chen, Y.Y. Gu, J. Li, E.M. Ding and Y.K. Shan, *Chem. Eur. J.*, **11**, 3894 (2005).
21. IUPAC, *Pure. Appl. Chem.*, **87**, 603 (1957).
22. T.W. Kim, R. Ryong, K. Michal, P.G. Kamil, J. Mietek, K. Satoshi and T. Osamu, *J. Phys. Chem. B*, **108**, 11480 (2004).
23. M. Kruk and M. Jaroniec, *J. Phys. Chem. B*, **106**, 4732 (2002).
24. R.R. Xu and W.Q. Pang, Molecular Sieve and Porous Material Chemistry, Sci. Publish. House, Beiing, p. 145 (2004).
25. D.Y. Zhao, J.L. Feng, Q.S. Huo, N. Melosh, G.H. Fredrickson, B.F. Chmelka and G.D. Stucky, *J. Am.Chem. Soc.*, **120**, 6024 (1998).
26. M. Kurk, M. Jaroniec, H.K. Chang and R. Ryoo, *Chem. Mater.*, **12**, 1961 (2000).
27. M.G. Song, J.Y. Kim, S.D. Cho and J.D. Kim, *Korean J. Chem. Eng.*, **21**, 1224 (2004).
28. M.C.R. Symons, *Acc. Chem. Res.*, **14**, 179 (1981).

(*Received*: 17 April 2008; *Accepted*: 15 January 2009) AJC-7116